

A New Torsion Balance for the Search of Long-range Interactions Coupling to Baryon and Lepton Numbers

Ramanath Cowsik, Dawson Huth, Tsitsi Madziwa-Nussinov

McDonnell Center for the Space Sciences at Washington University in St. Louis,
St. Louis MO

E-mail: cowsik@physics.wustl.edu

December 2020

Abstract. We have developed a torsion balance with a sensitivity about ten times better than those of previously operating balances for the study of long range forces coupling to baryon and lepton numbers. We present here the details of the design and expected characteristics of this balance. Operation of this balance for a year will also result in improved bounds on long range interactions of dark matter violating Einstein's equivalence principle.

1. Introduction

For over a century experimental efforts have probed Einstein's General Relativity (GR) theory; finding agreement with theoretical expectations at every turn [1]. However, the presence of dark matter and seeming incompatibility with the quantum theory of the Standard Model of Particle Physics (SM) leaves hollow a unified view of the universe. To address this, numerous theories have been proposed to bring GR and SM into a single framework at the cost of violating Einstein's Equivalence Principle (EEP) and introducing new particles or forces [2, 3], thus motivating experiments to search for a violation of the EEP. Also, after decades of direct and indirect dark matter searches revealing nothing [4, 5] EEP experiments are yet another route to gain insight into the nature of dark matter [6]

Some of the best modern tests of the EEP constrain the Eötvös parameter η which describes the validity of the universality of free fall (UFF). Terrestrial experiments using rotating torsion balances have placed upper bounds on composition-dependent forces in terms of the Eötvös parameter $\eta_{\text{Be-Ti}} = (0.3 \pm 1.8) \times 10^{-13}$ [7] and $\eta_{\text{Be-Al}} = (-0.7 \pm 1.3) \times 10^{-13}$ [8]. More recently torsion balance tests of the EEP have used chiral test masses probing violations of gravitational parity [9, 10] reporting $\eta_{\text{left-right}} = [-1.2 \pm 2.8(\text{stat}) \pm 3.0(\text{syst})] \times 10^{-13}$ [11]. The first results from the MICROSCOPE space based mission have reported $\eta_{\text{Ti-Pt}} = [-1 \pm 9(\text{stat}) \pm 9(\text{syst})] \times 10^{-15}$ [12].

Astronomical observations of a pulsar in a triple star system with two white dwarfs was also recently used to constrain η in the regime of the Strong Equivalence Principle (SEP), where contributions from massive self-gravitating test bodies can no longer be neglected. A. M. Archibald et al. [13] analyzed timing observations of the pulses from the pulsar over a six-year period showing that the relative accelerations of the white dwarfs and the neutron star varied by no more than a fraction $\sim 2.6 \times 10^{-6}$ of their mean accelerations or $\eta_{SEP} \sim 1.7 \times 10^{-5}$.

The possible existence of a 'dark/hidden sector' of particles which are neutral to the forces of the SM has been a leading motivation for Beyond Standard Model (BSM) physics searches and EP experiments are capable of probing the parameter spaces of these models [6]. Despite the sensitive bounds on η shown above plenty of untouched parameter space exists for future EEP violation searches to explore in the context of BSM physics and constrain properties of new particles of interest such as dark photons and Weakly Interacting Massive Particles (WIMPs) [14, 15].

The work presented here covers a recent 'pilot experiment' of the operation of a long-period torsion balance instrument sensitive to long-range forces coupling to baryon and lepton numbers. We discuss the subsequent instrument upgrades and the design of a new torsion balance developed to enhance our instrument's sensitivity to these forces. We conclude with the expected response of the new balance should the EEP be violated and prospects for placing lower bounds on η .

2. Pilot Experiment

The design of the pilot long-period torsion balance shown in Fig. 1 follows the classic design concepts developed by Dicke [16], Braginsky [17], and the more recent works of the Eöt-Wash group [8] and Zhu et al. [11]. The balance bob has four-fold azimuthal symmetry with 14.33 g test masses composed of Al and SiO₂. This symmetry significantly reduces the bob's coupling to gravitational gradients. The composition of the test masses were chosen to give large differences in baryon number per amu (B/μ), lepton number per amu (L/μ), and $((B - L)/\mu)$ thereby enhancing the bob's sensitivity to equivalence principle (EP) violating forces which couple to these charges [18]. Values for these parameters with respect to this pilot experiment, the Eöt-Wash group balance, and the new balance we have constructed can be found in Table 1. The composition dipole generated by these charge differences is subject to the gravitational field of the Sun and that of the dark matter halo centered about our Galactic Center. It is expected that any EP violating forces associated with those gravitational fields will exert a torque on the balance bob with a period of the length of the diurnal or sidereal day, respectively. Data acquisition with this instrument started on December 22, 2017 and continued until June 10, 2018 producing ~ 115 continuous days of useful data used in analysis. The balance bob's long natural period combined with the low frequency of the diurnal or sidereal signal cause long strings of uninterrupted data acquisition to be critical for the success of this instrument. This pilot experiment shows that collecting data of this kind

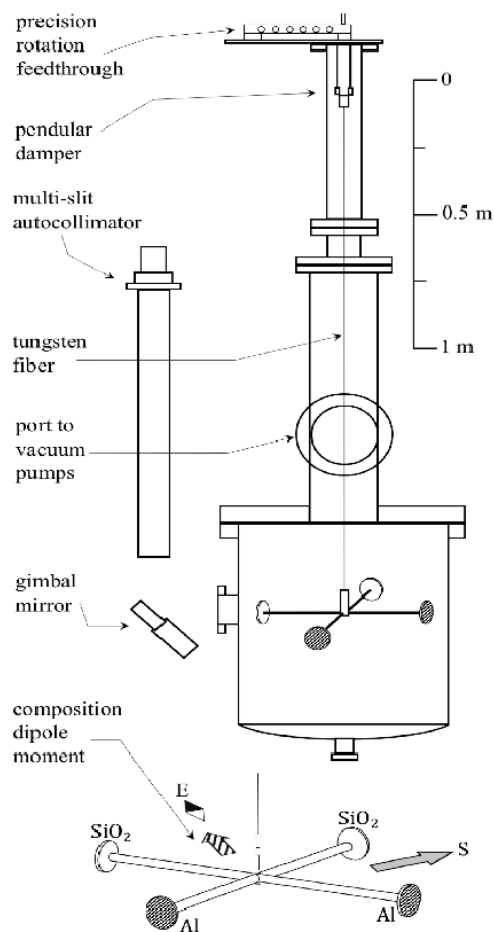


Figure 1: Line Drawing of the instrument used in the pilot experiment

is indeed possible.

In principle, a torsion balance of this design is significantly more sensitive to EP violating forces than the balance of the Eöt-Wash group but some noise sources were insufficiently addressed. Our instrument's pendular damper did not operate as efficiently as expected and large noise contributions in the low frequency regime of the balance's operation limited our final result. To address this thorough noise studies were performed to understand our instrument's response and various shielding techniques have been developed and implemented.

3. Noise Diagnostics and Remediation

We have studied the effects of the variations of Earth's magnetic field, absolute temperature and temperature gradient fluctuations, atmospheric pressure changes, and the instrument's support structure response to ambient seismic and thermal noise have been studied. In each noise study a length of ~ 2 weeks of the pilot balance's position and environmental data were collected. These data were then used in cross-correlation

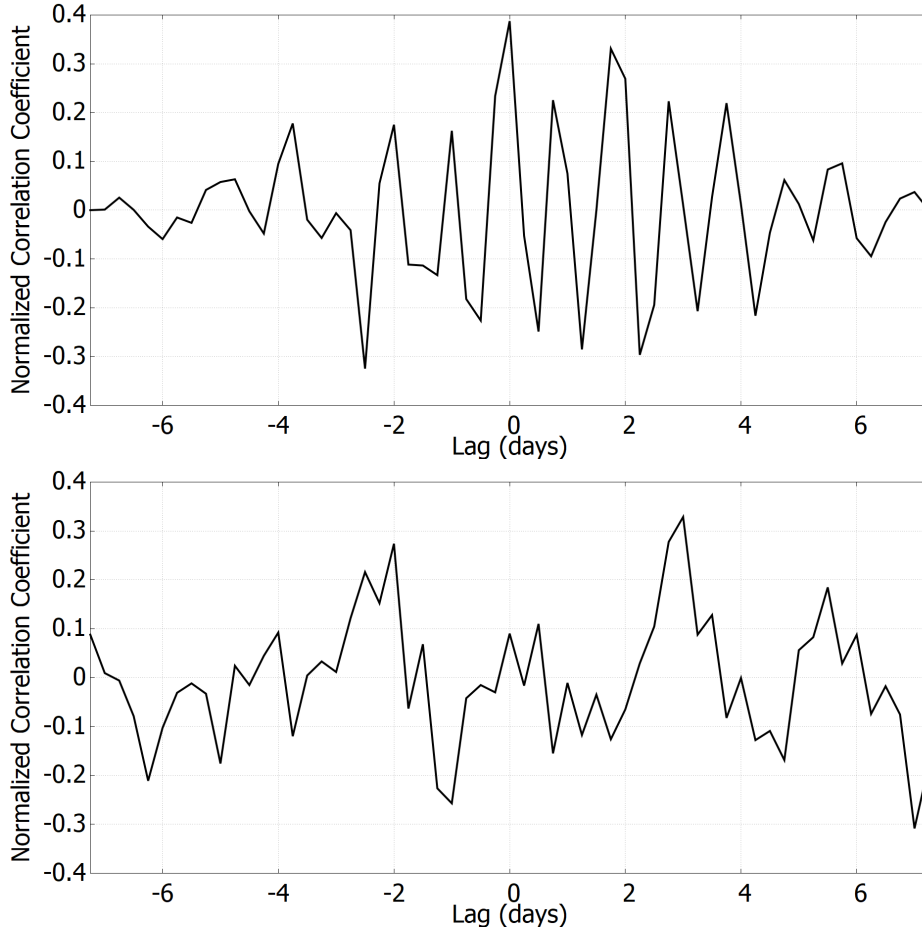


Figure 2: Plots of correlation coefficients between balance position and the Earth's magnetic field (top) and temperature gradients (bottom) in lag increments of 6 hours.

analysis where normalized correlation coefficients are calculated between the balance position and various environmental parameters under study. These coefficients are given by

$$R_{xy}(\tau) = \frac{1}{T} \int_{-T}^T \frac{(x(t + \tau) - \mu_x)(y(t) - \mu_y)}{\sigma_x \sigma_y} dt, \quad (1)$$

where R_{XY} is the normalized correlation coefficient between two sets of data x and y of length T calculated for some time lag τ between x and y . These data sets have means μ and standard deviations σ . This analysis showed that correlations with the Earth's magnetic field and variations in temperature gradients are the most significant noise contributions with normalized correlation coefficients of 0.4 and 0.3 respectively. Pressure variations yielded coefficients at the level of 0.01 and the coefficients for absolute temperature were also very low. Plots of the correlation coefficients as functions of time lag for the largest contributors are shown in Fig. 3.

Based on these studies we added magnetic shielding around the chamber and developed a water circulation system for evening out thermal gradients. For magnetic

shielding two layers of a woven low-carbon steel called G-IRON are used to completely surround the part of the vacuum chamber containing the balance. The woven structure of the material allows for sufficient pliability to be wrapped around the chamber without significant losses to magnetic permeability. Testing of this material showed good shielding performance with two concentric layers reducing the magnitude of the Earth's field measured with a magnetometer by about a factor of 40. To address the thermal gradient correlations a novel water circulation system was developed. Six air-to-water heat exchangers will surround the balance and be connected in series. A low power, ultra-quiet water pump connected to a large water tank will slowly circulate water through these heat exchangers evening out thermal gradients and reducing the amplitude of the diurnal thermal wave which propagates through the instrument. When the chamber is fully insulated with two layers of polyethylene foam, with the heat exchangers between the two layers, convection is the dominant heat transfer mechanism. With this in mind we expect significant reduction of thermal noise in the system.

4. Design of the New Balance

We are interested in detecting long-range forces which couple to baryon and lepton numbers so choosing test body materials which maximize these quantities is critical to a sensitive measurement of η . To this end a new balance was designed incorporating Cu and ultra-high molecular weight polyethylene (UHMWP). We ensured UHMWP is vacuum compatible by placing a sample with high surface area in a vacuum chamber separate from our instrument. The sample was pumped down to $\sim 10^{-8}$ torr within a day and reached a few parts in 10^{-9} torr after a few days giving a sufficient level of vacuum for our experiment without a prolonged outgassing period. Compared to the materials of the pilot balance this choice increases $\Delta(B/\mu)$ by over an order of magnitude; similarly $\Delta(L/\mu)$ and $\Delta(B - L/\mu)$ are enhanced by a factor of $\sim 6 - 7$ and these values can be compared with the Eöt-Wash balance in Table 1. Perusal of Table 1 also shows that this balance composition has a strong dipole moment for the three charge differences and one can note these charges for the Sun assuming a composition of 71% H and 29% He. The high (B/μ) and (L/μ) of the Sun relative to the surrounding interstellar medium and strong dipole moments of our balance will allow us to sensitively probe the coupling strengths for baryon-baryon and lepton-lepton interactions.

The balance is designed with a ring-shaped geometry where each semicircle has the same mass and the first and second order moments. The copper semicircle is comprised of four 90° arcs with two arcs stacked vertically on each half semicircle separated by ~ 1.5 cm. The UHMWP semicircle has two 90° arcs joined at the ends. The UHMWP semicircle is also covered with Cu foil to prevent the accumulation of patch charges and the entire assembly is joined with conductive epoxy. The higher azimuthal symmetry reduces couplings to gravitational gradients which induce spurious torques on the balance and also removes any preferential direction it may be deflected by radiometric flow compared to four-fold symmetric designs. We design for a mass of

530 g for larger coupling of any EP violating forces to the balance as well as reducing the response to torques suffered by the balance from radiometric flow inside the vacuum chamber. This flow is induced by temperature gradients across the vacuum chamber which we expect had a significant effect on the pilot balance. A picture of the assembled balance is shown in Fig. 3.

Characteristics	Eöt-Wash [7, 8]	Pilot	Current
Materials	Be-Ti	Al-SiO ₂	Cu-C ₂ H ₄
Total Mass (g)	70	72	530
Tine Length/Radius (cm)	2.01	25	25
Moment of Inertia (g cm ²)	3.78×10^2	3.75×10^4	2.96×10^5
Fiber Length (m)	1.07	1.67	1.67
Fiber Section	20 μm dia.	18 μm dia.	$15 \times 150 \mu\text{m}^2$
Torsion Constant (dyne cm rad ⁻¹)	2.34×10^{-2}	9.03×10^{-3}	7.93×10^{-2}
Natural Period (s)	798	12800	12100
Signal Torque (dyne cm)	3.98×10^{-12}	5.07×10^{-11}	3.98×10^{-10}
Expected Deflection (rad)	1.66×10^{-10}	5.62×10^{-9}	5.02×10^{-9}
Nyquist Torque (dyne cm)	3.14×10^{-12}	6.34×10^{-12}	1.84×10^{-11}
SNR (τ_S/τ_{Ny})	1.24	7.99	21.63
Balance Composition Characteristics			
$\Delta(B/\mu)$	2.2429×10^{-3}	1.2932×10^{-4}	2.2351×10^{-3}
$\Delta(L/\mu)$	1.5763×10^{-2}	1.6667×10^{-2}	11.3982×10^{-2}
$\Delta(B - L/\mu)$	1.3337×10^{-2}	1.8717×10^{-2}	11.6217×10^{-2}
Charge Composition of Sun	(B/μ)	(L/μ)	$(B - L/\mu)$
	0.9943	0.8493	0.1450

Table 1: Comparison of characteristics of our prototype instrument, proposed, and the Eöt-Wash instrument. Values for expected deflection, signal torque, and Nyquist torque assume an EP violation at the level of $\eta \sim 10^{-13}$ and an observation time of 10^7 s. The charge characteristics of the Sun are shown for reference

A thin tungsten fiber is used to suspend the balance because of tungsten's high tensile strength and large Q factor. The power spectral density of data from the pilot experiment is shown in Fig. 4 with a Lorentzian fit parameterized by a Q of 800 which is limited by the length of the data set. Tungsten has been shown to offer a Q factor up to 6000 by the Eöt-Wash group [7]. A data set much longer than the 100 days of observations that we had is needed to establish such a high value of Q for our balance with a natural period of $\sim 12,500$ seconds. A fiber of rectangular cross-section is used rather than a circular section. Circular section fibers with radius r have a torsion constant proportional to r^4 while a rectangular section is proportional to $a \cdot b^3$ where a is the width and b is the thickness of the tungsten strip. The rectangular geometry

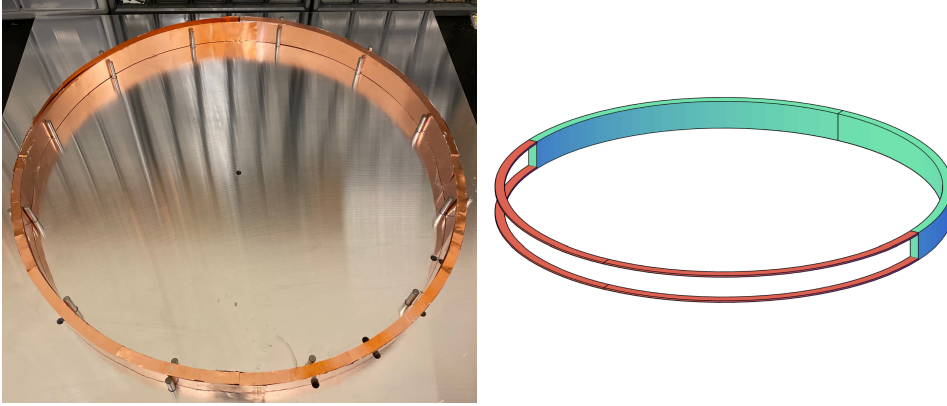


Figure 3: The constructed Cu-UHMWP balance on an aluminum jig used during assembly (left) and a 3D rendering of the balance test masses (right).

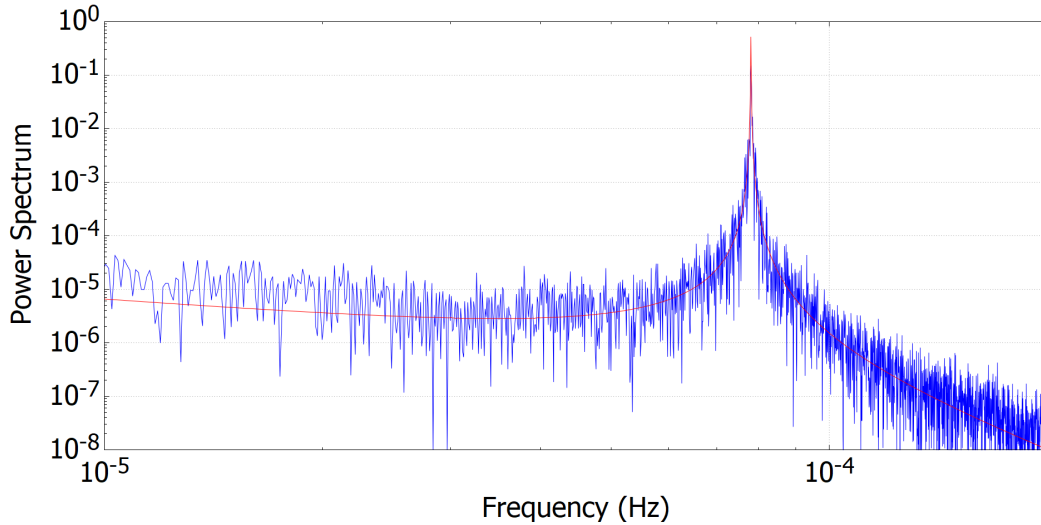


Figure 4: The power spectral density of 115 days of balance position data with a Lorentz fit parameterized with $Q = 800$. The peak is at the natural frequency of the pilot balance $\sim 7.8 \times 10^{-5}$ Hz.

allows for a sufficiently large cross-sectional area to support the more massive balance while only increasing the torsion constant of the fiber by a factor of ~ 8.8 rather than 60 for a circular section. The tungsten strip is attached to the disc of the pendular damper, which is suspended by a tungsten fiber of circular cross section, and as such reduces the sensitivity of the torsion balance to tilts. This leads to a similar expected deflection of 5×10^{-9} rad in the balance position for a given signal amplitude while increasing the SNR of the balance with respect to the Nyquist thermal noise in the suspension fiber by almost a factor of 3 compared to the pilot balance and a factor of ~ 17 compared to the Eöt-Wash balance.

5. Closing Remarks

Terrestrial experiments still hold much promise for measuring violations of the EEP to greater precision and the various motivations for new physics beyond the Standard Model fuel these efforts. In this work we have described past and current works searching for EP violations including a pilot experiment of a long-period torsion balance instrument. The lessons learned from this prototype have given us insight into where improvements can be made for better environmental isolation and a more sensitive torsion balance. Many of these changes have been implemented or are actively being developed and a measurement of η at the level of 10^{-13} or lower can be made.

6. Acknowledgements

We would like to thank the NSF for initial funding of this project, followed by funding from the McDonnell Center for the Space Sciences. We also recognize the earlier contributions of Michael Abercrombie, Adam Archibald, Maneesh Jeyakumar, Nadathur Krishnan, and Kasey Wagoner towards this effort.

References

- [1] Clifford M. Will. The confrontation between general relativity and experiment. *Living Rev. Rel.*, 9:3, 2006.
- [2] Thibault Damour. Theoretical aspects of the equivalence principle. *Classical and Quantum Gravity*, 29(18):184001, aug 2012.
- [3] Ephraim Fischbach, Daniel Sudarsky, Aaron Szafer, Carrick Talmadge, and S. H. Aronson. Reanalysis of the eoumltvös experiment. *Phys. Rev. Lett.*, 56:3–6, Jan 1986.
- [4] Felix Kahlhoefer. Review of lhc dark matter searches. *International Journal of Modern Physics A*, 32(13):1730006, May 2017.
- [5] Jennifer M. Gaskins. A review of indirect searches for particle dark matter. *Contemporary Physics*, 57(4):496–525, Jun 2016.
- [6] Sean Carroll, Sonny Mantry, Michael Ramsey-Musolf, and Christopher Stubbs. Dark-matter-induced weak equivalence principle violation. *Phys. Rev. Lett.*, 103:011301, 08 2009.
- [7] Stephan Schlamminger, Kwangyong Choi, T Wagner, Jens Gundlach, and E Adelberger. Test of the equivalence principle using a rotating torsion balance. *Phys. Rev. Lett.*, 100:041101, 03 2008.
- [8] T A Wagner, S Schlamminger, J H Gundlach, and E G Adelberger. Torsion-balance tests of the weak equivalence principle. *Classical and Quantum Gravity*, 29(18):184002, aug 2012.
- [9] Pedro Bargueño. Chirality and gravitational parity violation: True and false universal gravitational chirality. *Chirality*, 27, 04 2015.
- [10] N. D. Hari Dass. Test for c , p , and t nonconservation in gravitation. *Phys. Rev. Lett.*, 36:393–395, Feb 1976.
- [11] Lin Zhu, Qi Liu, Hui-Hui Zhao, Qi-Long Gong, Shan-Qing Yang, Pengshun Luo, Cheng-Gang Shao, Qing-Lan Wang, Liang-Cheng Tu, and Jun Luo. Test of the equivalence principle with chiral masses using a rotating torsion pendulum. *Phys. Rev. Lett.*, 121:261101, Dec 2018.
- [12] Pierre Touboul, Gilles Métris, Manuel Rodrigues, Yves André, Quentin Baghi, Joël Bergé, Damien Boulanger, Stefanie Bremer, Patrice Carle, Ratana Chhun, Bruno Christophe, Valerio Cipolla, Thibault Damour, Pascale Danto, Hansjoerg Dittus, Pierre Fayet, Bernard Foulon, Claude Gageant, Pierre-Yves Guidotti, Daniel Hagedorn, Emilie Hardy, Phuong-Anh Huynh, Henri

- Inchauspe, Patrick Kayser, Stéphanie Lala, Claus Lämmerzahl, Vincent Lebat, Pierre Leseur, Françoise Liorzou, Meike List, Frank Löffler, Isabelle Panet, Benjamin Pouilloux, Pascal Prieur, Alexandre Rebray, Serge Reynaud, Benny Rievers, Alain Robert, Hanns Selig, Laura Serron, Timothy Sumner, Nicolas Tanguy, and Pieter Visser. Microscope mission: First results of a space test of the equivalence principle. *Phys. Rev. Lett.*, 119:231101, Dec 2017.
- [13] Anne M. Archibald, Nina V. Gusinskaia, Jason W. T. Hessels, Adam T. Deller, David L. Kaplan, Duncan R. Lorimer, Ryan S. Lynch, Scott M. Ransom, and Ingrid H. Stairs. Universality of free fall from the orbital motion of a pulsar in a stellar triple system. *Nature*, 559(7712):73–76, Jul 2018.
- [14] Francesca Curciarello. Review on Dark Photon. *EPJ Web Conf.*, 118:01008, 2016.
- [15] Sarah Andreas. Update on Hidden Sectors with Dark Forces and Dark Matter. In *8th Patras Workshop on Axions, WIMPs and WISPs*, 11 2012.
- [16] P.G Roll, R Krotkov, and R.H Dicke. The equivalence of inertial and passive gravitational mass. *Annals of Physics*, 26(3):442 – 517, 1964.
- [17] V. Braginsky and V. Panov. Verification of the equivalence of inertial and gravitational mass. *Journal of Experimental and Theoretical Physics*, 34:463, 1972.
- [18] Thibault Damour. Testing the equivalence principle: why and how? *Classical and Quantum Gravity*, 13(11A):A33–A41, nov 1996.